Interactions of the B_3 cluster with H atoms and H_2 molecules

Ramon Hernandez and Jack Simons
Chemistry Department, University of Utah, Salt Lake City, Utah 84112

(Received 13 January 1992; accepted 24 February 1992)

Ab initio electronic structure calculations on several σ- and three-center bonded B_3H and B_3H_2 structures that correlate with the ground and first excited states of B_3 (plus H or H_2) have been carried out using correlation-consistent polarized valence double-zeta basis sets and complete-active-space self-consistent-field treatments of electron correlation. Geometries, electronic energies, and local harmonic vibrational frequencies were determined for two locally stable structures of B_3H and three stable and one metastable structures of B_3H_2 as well as for transition states connecting such structures. Reaction energies for several processes and a barrier for the $B_3 + H_2 \rightarrow B_3H_2$ reaction have also been calculated. A picture of the B_3 reactivity is given in terms of two coupled potential energy surfaces and their avoided crossings. The relevance of our findings to future experimental work and similarities with the chemistry of boranes and related reactive species are emphasized.

I. INTRODUCTION

In a recently published work,[1] we used *ab initio* quantum chemistry methods to predict the geometries, energies, and harmonic vibrational frequencies of several low-energy electronic states of the Boron trimer. The lowest two states have equilateral triangle geometries yet posess very different electronic structures. The $^2A_1'$ ground state has an electronic orbital occupancy (neglecting the three 1*s* core orbitals' six electrons) in which three B–B σ bonding orbitals (of a_1' and e' symmetry) are doubly occupied, a delocalized B–B–Bπ orbital (of a_2'' symmetry) is doubly occupied and a nonbonding orbital of a_1' symmetry shown in Fig. 1(a) is singly occupied. This orbital occupancy is denoted $1\sigma^2 2\sigma^2 3\sigma^2\ 1\pi^2 1n^1$. The lowest lying excited state is of $^2A_2''$ symmetry and is only 7000 cm^{-1} above the ground state and has an orbital occupancy of $1\sigma^2 2\sigma^2 3\sigma^2\ 1\pi^1 1n^2$. In this state, an electron is promoted from the $^2A_1'$ ground state's doubly occupied bonding π orbital shown in Fig. 1(b) to the nonbonding orbital of Fig. 1(a) to form the $^2A_2''$ state. As a result, the π orbital is half filled in the excited state and the nonbonding a_1' orbital is doubly occupied.

Because of the different orbital occupancy of these two low-energy states of B_3, one expects these two states to undergo quite different reactions; the ground state is a σ radical, and the excited state is a π radical. The study whose results are described here was undertaken to examine differences in reactivity for these two states of B_3 reacting with hydrogen atoms and the simple prototypical σ bond of the H_2 molecule. In carrying out this study, we were also interested in searching for stable B_3H and B_3H_2 geometries and transition states connecting these stable structures as well as in determining vibrational frequencies of such species to guide future spectroscopic studies.[2]

II. CHOICE OF ATOMIC ORBITAL BASIS SETS AND ELECTRONIC CONFIGURATIONS

A. Orbital basis set

The basis set for the boron and hydrogen atoms uses Dunning's correlation-consistent polarized valence double-zeta (CC-pVDZ) [9*s*4*p*1*d*/3*s*2*p*1*d*] and [4*s*1*p*/2*s*1*p*] bases,[3] respectively. The adequacy of the boron basis has been tested as detailed in our previous study of numerous electronic states of the boron trimer.[1]

B. Choice of electronic configurations

In forming a set of electronic configurations, one specifies a set of core orbitals that are doubly occupied in all configuration state functions (CSFs) as well as a set of valence orbitals among which the specified valence electrons are distributed. If the valence electrons are distributed in all possible ways, consistent with overall spin and spatial symmetry of the state of interest, one forms the set of complete active space (CAS) CSFs. This process is especially useful if sever-

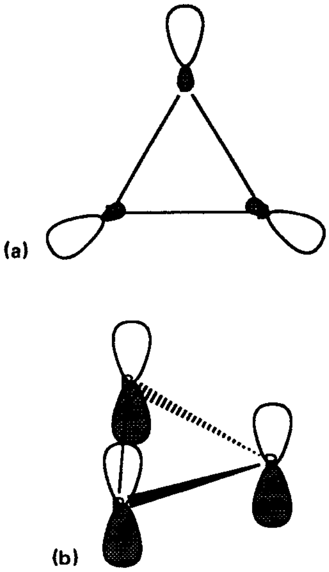

FIG. 1. (a) Nonbonding orbital of a_1 symmetry. (b) Delocalized π-type orbital of b_1 symmetry.

al different rearrangements of the molecular framework are to be studied as in the present study where two states of B_3, two stable B_3H structures and transition states connecting them, and several stable and transition-state B_3H_2 structures are under study.

Because of our interest in several structures, the choice of active valence orbitals for use in constructing our CSFs was guided by the following requirements:

(a) The CSF space must be flexible enough to properly describe at least the nondynamical correlation effects on the two lowest states (i.e., the above σ and π radical states) of the boron trimer because it is to these states that the states of B_3H and B_3H_2 studied here correlate at large interfragment distances.

(b) The CAS wave function should be capable of dissociating properly into the boron trimer and either one or two hydrogen atoms or a hydrogen molecule, depending on the chemical process being studied.

These conditions force one to include the three B–B σ bonding orbitals [labeled $3a_1$, $4a_1$, and $2b_2$ in C_{2v} symmetry appropriate to the most stable B_3H isomer identified here-see Fig. 2(a)], the delocalized 1π orbital (labeled $1b_1$), the nonbonding n orbital (labeled $5a_1$), the $6a_1$ and $3b_2$ orbitals for correlation as well as the one or two $1s$ orbitals of the one or two H atoms. As in our previous study, the $1s$ core $1a_1$, $2a_1$, and $1b_2$ orbitals of the boron trimer are doubly occupied in all CSFs. For B_3H the resulting eight active orbitals with their ten electrons give rise to 1176 total CSFs. For B_3H_2, there are eleven active electrons and nine active orbitals, which give rise to 6048 configurations of doublet spin symmetry.

III. RESULTS

A. Resulting qualitative molecular orbital structures

For the C_{2v} B_3H global minimum structure shown in Fig. 2(a), B–H bonding arises from the interaction of the $1n$ orbital in B_3 with the $1s$ orbital of the H atom and leads to a σ bond–antibond molecular orbital pair. For the higher-energy local minimum structure shown in Fig. 2(b), three-center B–H bonding arises from the interaction of the $1n$ and π orbitals of B_3 with the H atom's $1s$ orbital and produces a bonding, nonbonding, antibonding orbital trio.

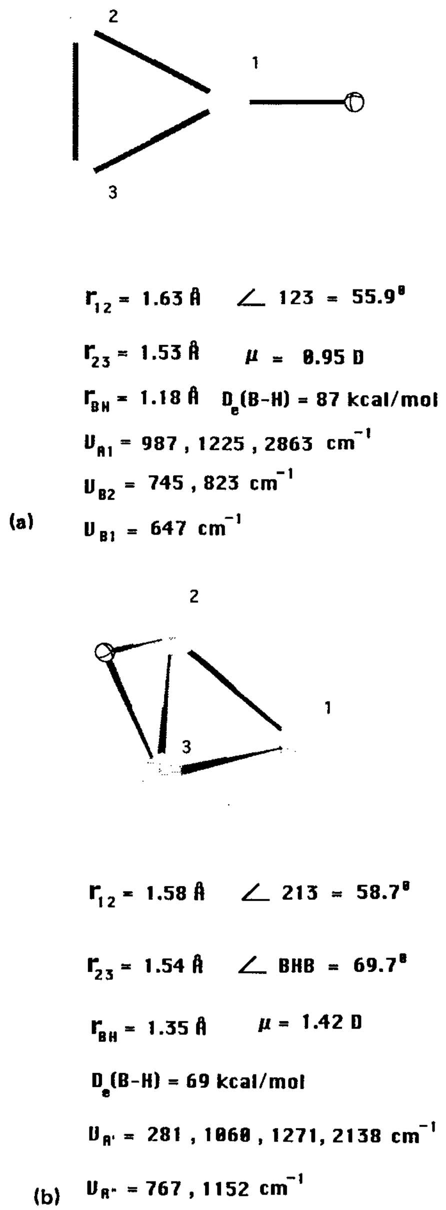

FIG. 2. (a) B_3H (σ-bonded) global minimum properties. (b) B_3H (π-bonded) local minimum properties.

B. B_3H stable geometries

We found two low-energy minima on the singlet B_3H potential energy hypersurfaces. The first, shown in Fig. 2(a), involves a single σ bond between the H atom and a B atom; it can be viewed as arising from simple radical coupling between the σ-radical $^2A_1'$ state of B_3 and an H atom. The geometrical parameters and local harmonic vibrational frequencies of this $^1A_1$ C_{2v} symmetry lowest-energy structure are also shown in Fig. 2(a). The dipole moment of this structure is 0.95 D, with the positive end of the dipole directed toward the H atom. The B–H bond strength of this species [i.e., the electronic D_e to form $^2A_1'$ B_3 and $H(^2S)$] is 87 kcal/mol. This bond strength can be compared with the recent accurate calculations[4] of the dissociation energy for diatomic BH (81.5 kcal/mol). Throughout this paper, the energy differences that are reported refer to *electronic* energies; only when explicitly stated are zero-point corrections included.

The second low-energy structure is of $^1A'$ symmetry in the C_s point group and has the geometry and vibrational frequencies detailed in Fig. 2(b). It has a three-center bridge bond involving two B atoms and the H atom, and is 19 kcal/mol less stable than the first structure discussed above. The dipole moment of this structure is 1.42 D, with the H atom again positive. This data suggests that the bridge-bonded H atom is more acidic than the terminally bonded H atom, which is a well known feature in borane chemistry.[5,6] The dissociation of the bridge-bonded structure to $B_3 + H$ is endoergic with $\Delta E = 69$ kcal/mol when ground-state B$_3$ is formed; it is endoergic by 89 kcal/mol if dissociation to the $^2A_2''$ π state of B$_3$ is considered. It should be mentioned that the bridge-bonded and terminally bonded structures both lie on the ground electronic state surface of the B$_3$H species, and both correlate to ground-state B$_3$ + H.

The bond lengths for the above low-energy structures are comparable with the terminal (1.20 Å) and bridge (1.32 Å) bond lengths found in diborane.[7] Also the symmetric stretching frequencies fall near the observed values for several boranes:[8,9] terminal B–H (2350–2630 cm^{-1}) and bridge B–H–B (1600–2220 cm^{-1}).

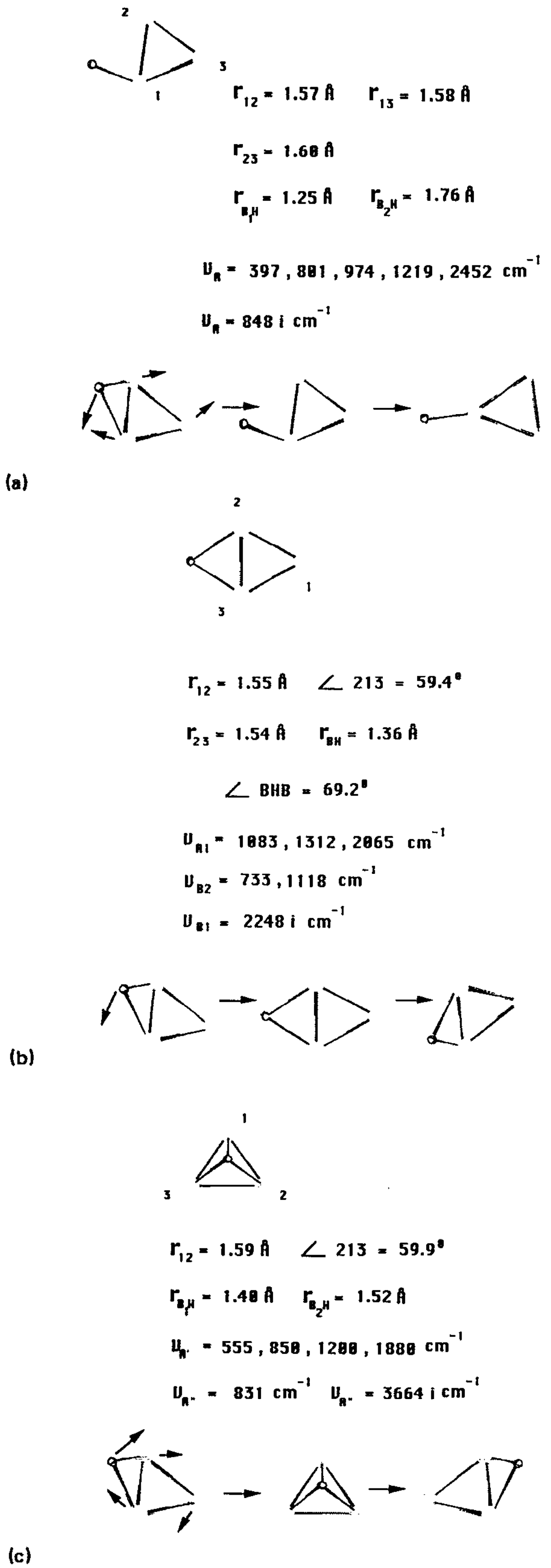

FIG. 3. (a) Transition state properties and reaction path for the interconversion of the σ-bonded and π-bonded species. The symmetry of the transition state is C_1. (b) Transition state properties and reaction path for the interconversion of equivalent π-bonded structures. The symmetry of the transition state is C_{2v}. (c) Transition state properties and lower energy reaction path for the interconversion of equivalent π-bonded structures. The symmetry of the transition state is C_s, *not* C_{3v}.

C. Interconversions among stable geometries of B$_3$H

Transition states (TSs) connecting the two types of stable geometries described above were also located and characterized by geometries, energies, and local harmonic vibrational frequencies. In Fig. 3(a) the reaction path connecting the three-center π-bridge-bonded C_s structure to the σ-bonded C_{2v} structure is pictured, and the geometric and other characteristics of the corresponding TS, which is of C_1 symmetry, are given. This TS lies only 1145 cm^{-1} (732 cm^{-1} or 2 kcal/mol when zero-point corrected) above the three-center-bonded structure. The interconversion of bridge and terminal hydrogen atoms has been previously studied in several boranes.[8,9] In particular Lipscomb[8] interpreted the boron NMR spectrum of B$_3$H$_8^-$ which showed equivalence of all boron atoms by assuming a pseudorotation path that permutes all of the hydrogen atoms with an estimated barrier of 0.8 kcal/mol.

In Fig. 3(b), we describe the reaction path connecting pairs of equivalent π-bonded C_s structures passing through a TS having C_{2v} symmetry. Along this path, which has a barrier of 2263 cm^{-1} (2083 cm^{-1} when zero-point corrected), the H atom moves from one side of the plane formed by the three B atoms to the other, preserving one σ_v symmetry plane throughout. Another path, which passes through a TS having C_s symmetry also connects pairs of equivalent π-bonded C_s structures yet has a barrier of only 979 cm^{-1} (302 cm^{-1} when zero-point corrected). This path is described in Fig. 3(c).

D. C_{3v} structures for B$_3$H

We examined the possibility that a C_{3v} structure could be geometrically stable, but we found that the lowest-energy electronic state for such structures posesses two negative curvatures (of E symmetry) that lead to spontaneous second order Jahn–Teller distortion. Close to the B$_3$ + H asymptote there is an avoided crossing (5 kcal/mol energy gap) between the two lowest-lying electronic states. The lower state leads to the above Jahn–Teller unstable state whereas the higher state (i) has a shallow minimum with a B–B internuclear distance of 1.60 Å and a B–H distance of 3.13 Å, (ii) lies only 856 cm^{-1} below the B$_3$ + H asymptote, and (iii) is unstable when zero-point energies are included. The avoided crossing results from the bonding interaction of the hydrogen atom with the singly occupied π orbital of B$_3$ (which

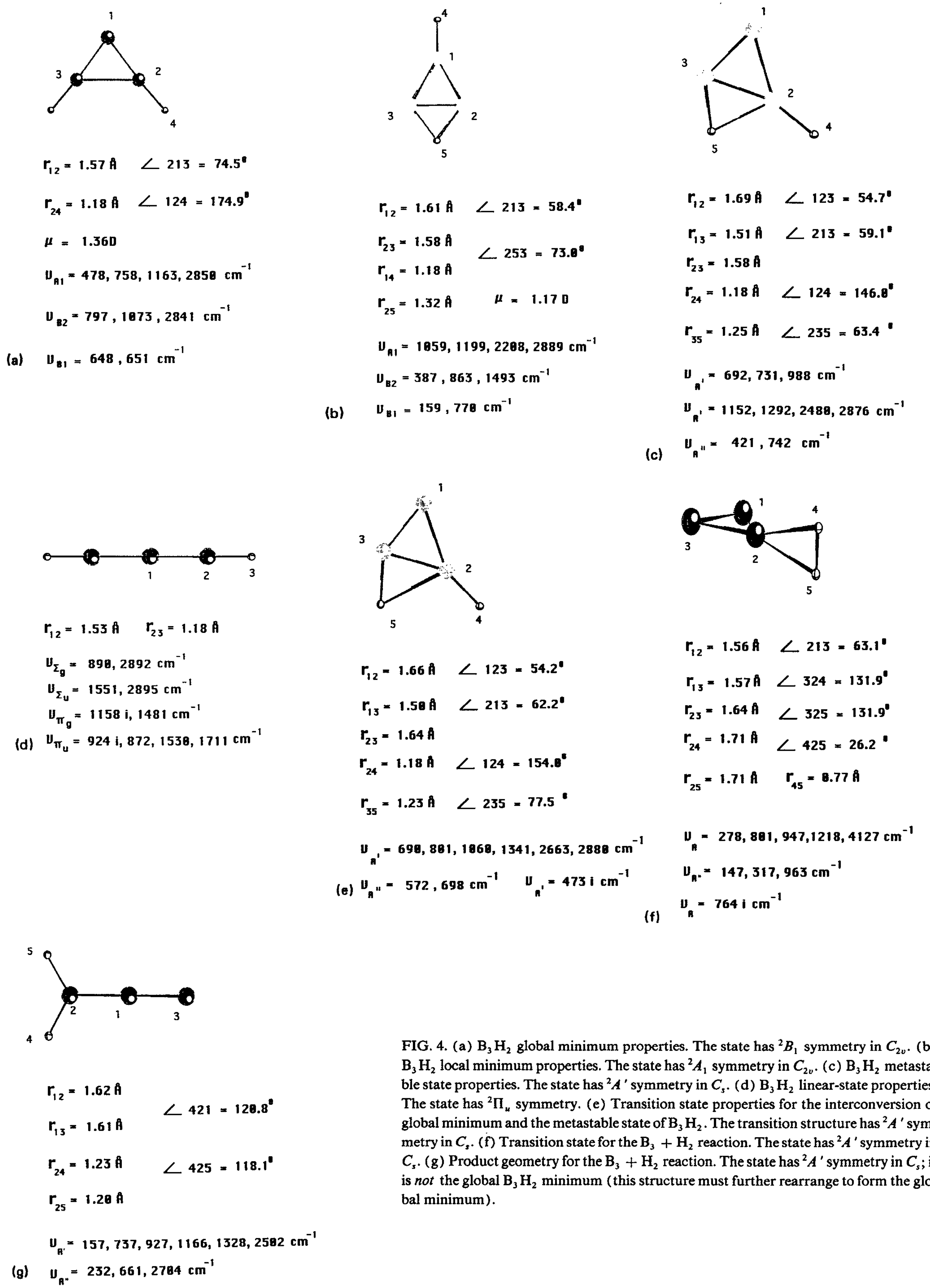

FIG. 4. (a) B_3H_2 global minimum properties. The state has $^2B_1$ symmetry in C_{2v}. (b) B_3H_2 local minimum properties. The state has $^2A_1$ symmetry in C_{2v}. (c) B_3H_2 metastable state properties. The state has $^2A'$ symmetry in C_s. (d) B_3H_2 linear-state properties. The state has $^2\Pi_u$ symmetry. (e) Transition state properties for the interconversion of global minimum and the metastable state of B_3H_2. The transition structure has $^2A'$ symmetry in C_s. (f) Transition state for the $B_3 + H_2$ reaction. The state has $^2A'$ symmetry in C_s. (g) Product geometry for the $B_3 + H_2$ reaction. The state has $^2A'$ symmetry in C_s; it is *not* the global B_3H_2 minimum (this structure must further rearrange to form the global minimum).

correlates with the first excited state of boron trimer) and the corresponding repulsive interaction when the π orbital is doubly occupied (which correlates with the ground state of the trimer). In C_{3v} both orbital occupations correspond to A_1 symmetry.

E. B_3H_2 structures

Four local minima were found for B_3H_2. The lowest-energy structure is depicted in Fig. 4(a), and corresponds to a bent structure having two terminal B–H bonds and a dipole moment of 1.36 D. This structure has $^2B_1$ electronic symmetry in the C_{2v} point group; the unpaired electron occupies an out-of-plane π-type orbital distributed over the three B atoms. Its geometry and local harmonic vibrational frequencies are given in Fig. 4(a).

A second locally stable structure is shown in Fig. 4(b), where its geometry and vibrational frequencies are given. It has one terminal B–H σ bond and one three-center B–H–B bridge bond and a dipole moment of 1.17 D. It has $^2A_1$ symmetry in the C_{2v} point group and lies 15 kcal/mol above the lowest energy structure. Its unpaired electron resides in an in-plane orbital localized on the two B atoms involved in the bridge bond.

Only 5.8 kcal/mol above the global minimum $^2B_1$ state is a linear $^2\Pi_u$ state [see Fig. 4(d)]. This degenerate state correlates with the lower-energy $^2B_1$ state mentioned above as well as with a state of $^2A_1$ symmetry when the molecule is bent. As can be seen from the harmonic vibrational frequencies this state presents Renner–Teller instabilities.

In addition to the two stable structures described above, we found a third local minimum that corresponds to a metastable state [see Fig. 4(c)] when zero-point energies are included. This structure has $^2A'$ symmetry and lies 25 kcal/mol above the lowest energy structure. This metastable state was found by following the lowest in-plane Hessian eigenmode starting at the $^2B_1$ global minimum passing through a transition state [see Fig. 4(e)] and finally going down to another local minimum (the metastable state). The electronic barrier height (measured from the local minimum) was found to be 173 cm^{-1} (when corrected for zero-point energies it becomes -161 cm^{-1}). Both transition and metastable states are characterized by having the unpaired electron in an in-plane orbital. The global minimum had the unpaired electron in an out-of-plane orbital and during the ascent to the transition state, out-of-plane vibrations accompanied by an avoided crossing allow the sharp change in electronic configuration.

The fourth local minimum structure was found when studying the insertion of the hydrogen molecule to the B_3 cluster and will be described in Sec. III G when this reaction path is reached.

When considered in C_s symmetry the global minimum is of $^2A''$ symmetry whereas the metastable state is $^2A'$. The fact that both states can be adiabatically connected, as was shown by walking from one to the other, suggests the presence of a conical intersection. Such an intersection can be found by symmetrically displacing the H atoms from the $^2B_1$ ($^2A''$) state. A crossing of $^2B_1$ ($^2A''$) and $^2A_1$ ($^2A'$) states occurs for B–H distances between 2.2–2.3 Å. This is to be expected since, at complete dissociation, the ground state of B_3 has $^2A_1$ symmetry and the first excited state is $^2B_1$.

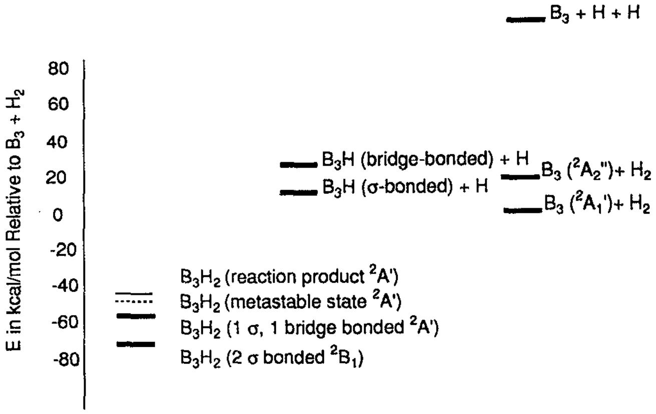

FIG. 5. Electronic energies of B_3H and B_3H_2 species relative to the ground states of B_3 and H_2.

F. B_3, B_3H, and B_3H_2 energetics

In Fig. 5 the relative electronic energies (without zero-point corrections) of the stable species described above are summarized. One observation which is important to make is that ground-state $B_3H + H$ is higher in energy than ground-state $B_3 + H_2$ by ca. 6 kcal/mol. This implies that the reaction of B_3 with H_2 to produce B_3H_2 can not, in the absence of tunneling and at room temperatures where $kT \cong 0.59$ kcal/mol, proceed through the stepwise abstraction of an H-atom to give $B_3H + H$ followed by the addition of a second H atom to yield B_3H_2. Therefore, the formation of B_3H_2 in its global ground state, which is a very exothermic reaction ($\Delta E = -78$ kcal/mol), must occur via a concerted process if at all.

G. Transition state for the $B_3 + H_2$ reaction

A variety of initial geometries representing possible approaches of the hydrogen molecule to ground state B_3 were investigated in order to find barriers to reaction. We found a transition state [see Fig. 4(f)] whose geometry is close to the reactant's as expected based on the Hammond postulate. In this transition state the hydrogen molecule is only slightly perturbed (0.770→0.775 Å) and the boron trimer has slightly lowered its symmetry (the largest change in bond length being 1.58→1.64 Å). The B_3 plane bisects the hydrogen molecule and is a plane of symmetry of the molecule. The unpaired electron is in an in-plane orbital similar to that in the ground state of the trimer. The electronic barrier height relative to $B_3 + H_2$ is only 4.6 kcal/mol so that zero-point effects become very relevant. The zero-point corrected barrier height is 6.8 kcal/mol. We have not considered the basis set superposition error but its effect should be to slightly increase the barrier height.

Moving down from the transition state to products, we observe the breaking of the H–H and one B–B bond while forming two terminal B–H bonds. The formation of B–H bonds is accompanied by the breaking of the π-type bond in B_3, which is responsible for the relative stability of ring over linear structures in the isolated B_3 fragment. One of the boron atoms involved in the bond-breaking process [atom #3 in Fig. 4(f)] executes a large amplitude motion until it finally reaches the minimum structure depicted in Fig. 4(g)]. Here, the unpaired electron resides mainly in a p-type orbital on the terminal boron atom directed collinearly with all boron atoms. This minimum lies 27.9 kcal/mol above the global B_3H_2 ground state. It can be thought of as correlating with one component of the $^2\Pi_u$ state of linear B_3. A low-lying excited state correlating with the other degenerate component of $^2\Pi_u$ is observed at 55.3 kcal/mol relative to the B_3H_2 global minimum (this estimate uses the CI energy of the first excited state with the orbitals optimized for the ground state), which is also bound with respect to ground-state $B_3 + H_2$.

H. Related work

The chemisorption of hydrogen onto metal and semiconductor surfaces has been the subject of a considerable amount of theoretical research using cluster models.[10,11] In particular, chemisorption onto boron surfaces was the subject of a previous *ab initio* study.[12] In that work, a six-membered cluster was fixed in the shape of a capped pentagon structure and a variety of paths describing the approach of H_2 to this cluster were considered. The main objective of that study was to find paths that lead to chemisorbed hydrogen, but not necessarily to minima that require major rearrangement of the boron lattice structure.

Our work concentrates on properties of the clusters, not as they represent fragments of a surface. As has been previously emphasized,[13] the behavior of clusters such as we are studying can be quite different from those of cluster fragments of surfaces. In particular, we find that terminal boron–hydrogen bonds are stronger than bridge or threefold bonds whereas in the cluster-model study the terminal bonding is not even considered.

The fact that terminal bonds play an important role in the interaction of boron clusters with hydrogen is consistent with the recent experimental results of a collisionally induced dissociation study of boron cluster cations with deuterium and deuterated water.[14] Formation of both B_3D and B_3D_2 positive ions has been observed. In that work, the resultant boron-deuterium bond energies compare well with our *terminal* B–H bond energies. The B–H bond energies coming from the cluster-model study are smaller. Although quantitative differences between aluminum and boron clusters have been noted,[14] the low aluminum–hydrogen binding energies (corresponding to bridge and threefold bonds) reported in a recent work[15] suggest that again only local, as opposed to global, minima were found.

Finally, evidence to support the high mobility of hydrogen atoms for movements parallel to a boron surface predicted by the previous cluster-model study is also observed in the present study.

IV. SUMMARY AND CONCLUSIONS

The $B_3 + H_2$ system has been described in terms of two coupled potential surfaces which produce, in their dissociation limits, the ground state hydrogen molecule and the ground and first excited states of B_3. The lowest energy linear states of the boron trimer have also been shown to play roles in the description of the ground state surface of B_3H_2. Geometries, local harmonic vibrational frequencies, and dipole moments of two stable B_3H species and three stable and one metastable B_3H_2 species have been predicted based on these calculations.

Vibronic coupling effects have been identified in the form of Renner–Teller instabilities, conical intersections, and avoided crossings. The latter are directly related with the ability of the B_3 cluster to behave as a sigma or pi radical and to allow the system to change electronic configuration as a function of geometry. The fact that the ground surface presents a conical intersection allowing the adiabatic linkage of states of different symmetry could, in principle, have spectroscopic and dynamical signatures. Unfortunately for a five atom system the situation is more complicated than, for example, the well-known rule of fractional quantization of pseudorotation for triatomic systems[16] so that we cannot make any specific predictions at this time, however, we hope this information can be used for interpretive purposes in future experimental studies.

The hydrogen abstraction reaction $B_3 + H_2 \rightarrow B_3H + H$ is found to have an endothermicity of 6 kcal/mol. Assuming that an additional dynamical barrier for this process of at least 1 kcal/mol exists, the direct $B_3 + H_2 \rightarrow \mathrm{TS} \rightarrow B_3H_2$ addition of a hydrogen molecule is predicted to be the lower energy reaction path for the $B_3 + H_2$ system. The barrier for the latter process is 6.8 kcal/mol.

Two stable isomers of B_3H were studied. Their interconversion, as detailed in this work, could be used as a simple model for the bridge to terminal hydrogen exchange present in some boranes and related inorganic reactive species. The low barriers to interconversion of equivalent bridge-bonded structures should be reflected in the tunneling splittings observed in vibrationally resolved spectra.

ACKNOWLEDGMENTS

This work was supported in part by the Office of Naval Research and by the National Science Foundation Grant No. CHE8814765. We also thank the Utah Supercomputer Institute for staff and computer resources.

[1] R. Hernandez and J. Simons, J. Chem. Phys. **94**, 2961 (1991).

[2] (a) Z. Fu, G. Lemire, Y. Hamrick, S. Taylor, J. Shui, and M. Morse, J. Chem. Phys. **88**, 3524 (1988); (b) Y. M. Hamrick, R. J. Van Zee, and W. Weltner, J. Chem. Phys. **95**, 3009 (1991).

[3] T. H. Dunning, J. Chem. Phys. **90**, 1007 (1989).

[4] C. Bauschlicher, S. Langhoff, and P. Taylor, J. Chem. Phys. **93**, 502 (1990).

[5] *Boron, Metallo-boron Compounds and Boranes*, edited by R. Adams (Interscience, New York, 1964).

[6] W. N. Lipscomb, *Boron Hydrides* (Benjamin, New York, 1963).

[7] *Gmelin Handbuch der Anorganischen Chemie* (Springer, Berlin, 1978).

[8] W. N. Lipscomb and M. L. Mckee, Inorg. Chem. **21**, 2846 (1982).

[9] H. Horn, R. Ahlrichs, and C. Kolmel, Chem. Phys. Lett. **150**, 263 (1988).

[10] M. Simonetta and A. Gavezotti, Advan. Quantum Chem. **12**, 103 (1980).

[11] *Theory of Chemisorption*, edited by J. R. Smith (Springer, Berlin, 1980).

[12] B. Sykja and S. Lunell, Surf. Sci. **141**, 199 (1984).

[13] (a) J. Koutecky and P. Fantucci, Chem. Rev. **86**, 539 (1986); (b) V. Bonacic-Koutecky, P. Fantucci, and J. Koutecky, Chem. Rev. **91**, 1035 (1991).

[14] (a) S. Ruatta, L. Hanley, and S. L. Anderson, J. Chem. Phys. **91**, 226 (1989); (b) P. Hintz, S. Ruatta, and S. L. Anderson, J. Chem. Phys. **92**, 292 (1990).

[15] (a) T. H. Upton, D. M. Cox, and A. Kaldor, *Physics and Chemistry of Small Clusters*, edited by P. Jena, B. K. Rao, and S. N. Khanna (Plenum, New York, 1987), p. 755; (b) T. H. Upton, Phys. Rev. Lett. **56**, 2168 (1986).

[16] (a) G. Delacretaz, E. Grant, R. Whetten, L. Woste, and J. Zwansiger, Phys. Rev. Lett. **56**, 2598 (1986); (b) C. A. Mead and D. G. Truhlar, J. Chem. Phys. **70**, 2284 (1979).